Preprints (www.preprints.org) | NOT PEER-REVIEWED | Posted: 14 October 2020

Article,

Cement composition's effect on pore solution composition and on electrochemical behavior of reinforcing steel

Amit Kenny [1,*] and Amnon Katz [2]

[1] Department of Civil Eng., Shamoon College of Engineering, Ashdod, Israel; amitke@sce.ac.il
[2] Faculty of Civil Eng., Technion – Israel Institute for Technology, Haifa, Israel; akatz@technion.ac.il
* Correspondence: amitke@sce.ac.il;

Abstract: Reinforcement corrosion due to chloride attack is of major economic significance for reinforced concrete structures. Pozzolans are known to inhibit corrosion initiation mainly by reducing concrete permeability. However, there is evidence in the literature that changes in the chemical environment in the concrete due to the pozzolans may be creating improved corrosion resistance, by themselves. In this study, the composition of a pore solution of mature hydrated cement paste containing silica-fume at different ratios was analyzed. The electrochemical behavior of reinforcing steel was studied in simulated pore solutions with silicate concentrations ranging from 0 to 35.6 mM, which are within the concentration range found by pore solution extraction to be up to 49 mM. Polished reinforcing steel specimens were used for cyclic voltammetry in simulated pore solutions with chloride concentrations of 10-20%. Better corrosion protection was found with increasing silicate concentration up to 3.56 mM. This was indicated by lower corrosion currents both in the passive state and after anodic activation. Anodic activation of steel in a 35.6 mM silicate solution with 20% NaCl yielded a higher potential than the anterior potential.

Keywords: concrete; pore solution; silica; pozzolan; corrosion; cyclic voltammetry; silicate; corrosion inhibition

1. Introduction

Corrosion of reinforcing rebars of reinforced concrete (RC) structures (RCS) is the limiting factor of the usable life expectancy of RCS, and has a major economic impact [1], [2]. The reinforcing steel embedded in intact concrete is in a passive state, i.e. the corrosion rate is negligible. The deterioration due to reinforcement corrosion is a result of a two stage process. The first stage is depassivation of the reinforcement due to chloride ingress or carbonation. The second stage is reduction in rebar cross section and corrosion-induced cracking as a result of corrosion product crystallization pressure. The time to depassivation of the reinforcement depends on the permeability of the concrete, and the critical chloride threshold. Each of these was studied separately.

There are several methods for investigating RC corrosion. These include autopsy of existing RCS [3], [4], investigation of specimens of embedded steel in concrete [5], [6], [15]–[21], [7]–[14], analysis of embedded steel in mortar [14], [15], [20], [22]–[25], and of steel in pore solutions [5], [26]–[32]. The corrosion assessment is usually done by electrochemical methods, but mass loss is also common. Following are the advantages and disadvantages of studying the various types of specimen. Electrochemical methods will be shortly reviewed later.

The studies of reinforcement corrosion in concrete should simulate the corrosion of RC in the most accurate way. Some studies have investigated only the time to corrosion initiation [8], [33]–[35], which is the overall result of the process involving chloride diffusion and steel depassivation, ignoring the mechanisms of corrosion initiation. There are several disadvantages to using concrete for the investigation: 1. The concrete cover has to be bigger than the maximum aggregate nominal size. This leads to a long time for chloride diffusion for corrosion initiation, and extends the duration of the investigation. 2. Many parameters of the concrete mix are interdependent, i.e. changing one

© 2020 by the author(s). Distributed under a Creative Commons CC BY license.

Preprints (www.preprints.org) | NOT PEER-REVIEWED | Posted: 14 October 2020

parameter changes another. This impairs the ability to infer causation from the correlation between mix properties and the corrosion mechanism. 3. Local variability of parameters is high [36]. This reduces the quality of correlations achieved. For these reasons, many investigators have studied the corrosion process in simplified mediums, such as mortar, paste or simulated pore solution.

Using mortar allows a significant reduction of the cover on the reinforcement, which leads to a shorter diffusion process and a shorter investigation time. However, there is evidence that the steel-concrete interface (SCI) plays an important role in corrosion initiation in mortar as it does in concrete [37]. The SCI is a parameter which is not fully controlled yet [38]. The SCI itself may cause high variation in results. It has been demonstrated that variation in the SCI alone may cause variation of the critical chloride threshold for corrosion initiation to the extent of the range reported in the literature [36]. Hence, to separate the chemical effects of the pore solution composition from those of the chemistry and microstructure of the hardened cement paste, an investigation of the corrosion process in simulated pore solution is preferred.

Most reported studies involving simulated pore solution have used saturated calcium hydroxide solution with an addition of sodium/potassium hydroxide for pH adjustment to a pH of 12.4 and above [5], [26]–[32]. These studies were the first to point out the important parameters of the effect of steel surface condition [39] and specimen size [40]. Nevertheless, a solution of calcium and sodium hydroxides is a simplification of the pore solution. An actual pore solution contains additional minor ingredients which may vary depending on the cement composition and can have a significant effect on the corrosion of the steel.

Only a few studies have measured the pore solution composition of cement paste. Of those, fewer still have measured the concentration of ions in mature paste. In those studies, a one-fold concentration difference was found between ordinary Portland cement (OPC) and white Portland cement [41]; different concentrations were reported for activated alkali-activated ground granulated blast-furnace slag [42], limestone or fly-ash blended cement [43]–[47]. Thus, pore solutions differ in more parameters than simply their pH, and these parameters have a relation to cement composition and an influence on corrosion which have not previously been studied.

Cement composition in respect of reinforcement corrosion has mainly been researched in the context of C_3A content, alkalinity, and blended material content. Most papers have focused on concrete permeability and the apparent chloride diffusion coefficient [8], [34], [35]. Researchers investigating the chloride threshold in concrete have not found a definitive result, with some investigations finding a reduced chloride threshold [48] and others a higher one [49]. This may be a consequence of other parameters which affect the chloride threshold, such as steel condition and the steel-concrete interface, which can cause a high variation in results. Researchers who reduced variation by investigating the chloride threshold of steel in simulated pore solution have focused on the pH of the solution, assuming that pozzelanic blended cements have only a lower pH [49].

A study, originating from the observation that on-shore RCS with alkali-silicate reaction (ASR) induced cracks have less corrosion than other on-shore RCS, led to the finding that the materials which cause the ASR lead to better passivation of the reinforcing steel [3]. These materials are similar to the pozzelans, which contain amorphous silicate. This hints that the silicate in the pozzolans may play a role in the passivation of reinforcing steel. The orthosilicate anion and its acids ($H_xSiO_4^{(4-x)-}$,$0<x<3$) are large multivalent ions; as such they are preferentially adsorbed on solid surfaces including steel oxidation products instead of hydroxide and chloride ions [50], [51]. In the case of iron oxidation, a high silicate concentration at a high pH will result in ferrum silicate deposition, which is insoluble to pH as low as 2. A study in a pH=12 environment found a dense layer of silica forming on an anodic steel surface [51]. Both layers may result in a passivation layer, which could be more durable than the ferrum hydroxide. In environments which are not simulate concrete pore solution, silicate was found to improve steel corrosion resistance [51]–[57]; it is used as inhibitor in the process industry [51], [58]. The above-mentioned information hints that pozzolans in concrete may have a chemical effect on the corrosion resistance of reinforcements.

There are several electrochemical methods used for studies of corrosion. The more common methods are: electrochemical potential (EP), linear polarization (LP), electrochemical impedance (EIS), and cyclic voltammetry (CV). Following is a short review of these.

Preprints (www.preprints.org) | NOT PEER-REVIEWED | Posted: 14 October 2020

The EP is the electrical potential of the steel, relative to a reference electrode. Reduction in the EP is a hint of a change in the passivation layer, which may be a depassivation, i.e. initiation of active corrosion. Many studies of RC corrosion use EP tracking. The disadvantages of the method are: (1) reduction of potential is not necessarily caused by depassivation; and (2) this indicator gives no information regarding the process of depassivation or the corrosion rate.

EIS is a relatively new technique. By measuring a spectrum of impedance along a frequency range, an equivalent circuit can be inferred and parameterized. One of the components of such a circuit is the electrical resistance of the passivation layer. The transformation from passive to active corrosion is a result of a drop in the resistance of the passivation layer, which can be measured by EIS. Thus, EIS gives information which is directly related to the corrosion state.

LP is a controlled change of the EP around its open circuit potential (OCP). The current and potential are recorded. The typical potential range is ±20 mV from the OCP. The corrosion rate at the OCP can be estimated from the results by using the Stern-Geary equation [59].

In CV, the EP is gradually changed from -20 mV below the OCP up to where active corrosion is achieved. Then, the potential is gradually changed down to one which is much lower than the original OCP potential. The received diagram contains two sections of LP, one for the ascending and the other for the descending potentials. If the investigated specimen starts at a passive state, the LP in the ascending phase gives the OCP and its corrosion rate at the passive state. The increase in potential forces initiation of pitting in the specimen. The LP in the descending potential section gives the pitting corrosion current and its OCP.

Accordingly, a CV gives the EP in both the active and passive states, saving the time and uncertainty of an EP vs. time measurement and making it redundant; it enables a controlled change from the passive to the active state; and it includes corrosion current as the LP and EIS. These advantages make the CV technique an adequate method for the study of the inhibition effect of pore solution chemistry in a simulated pore solution.

Because of the complexity of the RC corrosion process, the study of the chemical influence of pozzolans on the corrosion of reinforcing steel cannot be conducted in concrete. The electrochemical behavior of steel has to be studied in a simulated pore solution. In order to produce an accurate simulation of a pore solution of concrete with different pozzolan contents, the pore solution of different pozzolan contents has to be analyzed first. In this work, a pore solution of cement paste with different silica fume contents is analyzed; it serves as a model for the pozzolans. The electrochemical behavior of reinforcing steel was studied in a simulated pore solution with varying silicate concentrations, based on the concentrations found in the pore solution. Additional data, which is irrelevant for RC corrosion but may be of value for other studies, is presented in the appendixes.

2. Materials and Methods

2.1. Materials

Nine pastes were prepared consisting of CEM I 52.5 N (EN-197, by Nesher ltd. Israel), silica-fume (grade 940 by Elkem Norway), limestone powder (Avgil 510 by Microgil Israel), and tap water. Paste compositions are presented in Table 1. Material compositions are presented in Table 2 - Table **4**. The SF was used to model pozzelanic materials, and the limestone powder was used to prevent segregation. The pastes were cast into 50 ml centrifuge tubes and tapped. The tubes were maintained in standard laboratory conditions until the pore solution extraction, at an age of 6-9 months.

Table 1. Compositions of pastes

Notation	Cement	Water	Limestone powder	Silica-fume
SF0	1000	650	350	0
SF5	1000	650	300	50
SF10	1000	650	250	100
SF15	1000	650	200	150
SF20	1000	650	150	200

Preprints (www.preprints.org) | NOT PEER-REVIEWED | Posted: 14 October 2020

SF25	1000	650	100	250
SF30	1000	650	50	300
SF35	1000	650	0	350
SF40	1000	650	0	400

Table 2. Cement composition

Component	% (w/w)
CaO	62.49
SiO_2	18.73
Al_2O_3	5.37
Fe_2O_3	3.61
MgO	1.13
TiO	0.35
K_2O	0.45
Na_2O	0.21
P_2O	0.45
Mn_2O_3	0.04
SO_3	2.55
LOI 600	1.26
LOI 950	3.16
LOI total	4.42

Table 3. Silica fume composition (manufacturer data)

Component	% (w/w)
SiO_2	>90%
H_2O	<1%
LOI	<3%

Table 4. Limestone powder composition (manufacturer data)

Component	% (w/w)
$CaCO_3$	99.4
SiO_2	0.20
MgO	0.06
Fe_2O_3	0.02
Al_2O_3	0.05
SO_3	0.03
H_2O	0.27
LOI	43.60

2.2. Pore solution extraction

The pore solution was extracted using a device built according to Barneyback and Diamond [60]. The force applied on the piston was 270 kN. The quantity of pore solution extracted was about 2 ml (deduced by weighing the specimen before and after extraction). The extracted solution was collected by syringe, and filtered through a 220 nm filter, to remove solids which may dissolve or harm the analytical equipment.

2.3. Chemical analysis

The pore solution was diluted at 1:10 in deionized water to achieve sufficient volume for the chemical analysis. Ion content of the dilute solution was measured by ICP.

Preprints (www.preprints.org) | NOT PEER-REVIEWED | Posted: 14 October 2020

The pH of the dilute solution was measured by ISE. The pH of the pore solution was calculated based on the pOH and the dilution, according to the following equations:

$$[OH]_{pore\ solution} = [OH]_{measured}/dilution \quad (1)$$

$$pOH = 14 - pH \quad (2)$$

$$pOH = -\log([OH]) \quad (3)$$

A procedure for method validation and validation results is described in Appendix A.

2.4. Synthetic pore solution

In order to measure the electrochemical behavior of reinforced steel in a pore solution, an artificial pore solution was prepared by dilution of sodium silicate (water-glass) to obtain the desired Si concentration with NaOH added for pH correction. The silicate concentrations were 0, 0.356, 3.56, and 35.6 mM (as Si). The pH was fixed to 13, in order to reduce the variability to that of only the silicate concentration.

2.5. Specimen preparation for CV

Steel specimens were prepared by milling reinforcing steel to a diameter of 10 mm and a length of 20 mm. To the backs of each steel cylinder an electrical wire was attached. The cylinders were rinsed with acetone, dried in hot air, and soaked in a silicate solution of 35.6 mM and pH 13 for 24 hr. Later, the cylinders were rinsed in deionized water and acetone and dried in hot air. The cylinders were inserted into molds with a centering groove for a vacuum epoxy cast. The front of the specimens was polished to 800 grit. Three specimens were prepared for each concentration.

2.6. Electrochemical measurement – CV

The electrochemical behavior of the steel in the simulated pore solution was studied by Cyclic Voltammetry (CV). In this method, the specimen potential, V, is brought to a potential which is somewhat lower than the OCP potential—in this work to 0.1 V below the OCP. Then the potential is gradually raised to a potential in which oxidation is certain to occur. Next, the potential is gradually reduced to a potential which is much lower than the OCP potential: to -1 V vs. saturated calomel electrode (SCE) in this work. During the controlled changes in potential, the current, I, needed to maintain each potential is recorded. The result is a V vs. log(I) diagram.

The resulting V vs. log(I) diagram can be analyzed to yield the corrosion current in the OCP, the pit initiation potential, and with pit area, the in-pit corrosion current [61].

Preliminary results showed that increase of the potential caused thickening of the passivation layer and no pit initiation. NaCl was added to the silicate solution to allow pitting. The NaCl concentrations which were used in the final investigation are shown in Table 5.

For each electrochemical test, three specimens were used.

Experiments using other electrochemical methods prior to selecting the CV method are detailed in Appendix C.

Table 5. Final NaCl concentrations in the silicate solutions for CV investigation

Silicate [ppm (Si)]	[Si] (mM)	NaCl [% w/w]
0	0	10
10	0.356	10
100	3.56	15
1000	35.6	10, 15, 20

3. Results

Preprints (www.preprints.org) | NOT PEER-REVIEWED | Posted: 14 October 2020

3.1. Pore solution

The composition of the pore solution is presented in **Table 6**. The silicate concentration increases by two orders of magnitude from 0.294 mM for no SF addition to 49 mM for a 20% SF addition. Then it decreases to 3.4 mM for a 40% SF addition (**Figure 1**). The pH decreases slightly with the addition of SF of up to 10% of cement weight. With greater additions there is no clear trend. The lowest pH found is 11.44 for a 15% SF addition. Ca concentration ranges from 0.343 mM for no SF addition up to 2.488 mM for a 30% SF addition, with no clear trend. The alkalis, K and Na, show a generally decreasing trend with increasing SF content with the exceptions of SF20 and SF25 which slightly deviate from this trend. The K/Na ratio decreases from 1.3 for SF0 to 0.9 for SF15, and rises back to 1.2 from SF25 and on.

Table 6. Pore solution composition for hardened cement paste mix

Notation	% SF of cement	pH	Ca (mM)	Si (mM)	Al (μM)	Fe (μM)	Mg (μM)	K (mM)	Na (mM)
SF0	0	13.55	0.343	0.294	223.6	11.69	7.94	176.7	133.7
SF5	5	13.13	1.218	1.720	18.7	0.87	0.00	67.2	71.3
SF10	10	12.86	1.508	0.414	27.8	5.23	19.30	34.6	37.8
SF15	15	11.44	0.927	14.861	15.6	3.20	1.36	32.2	36.1
SF20	20	12.50	1.432	49.124	34.9	1.59	4.77	41.9	45.3
SF25	25	11.76	0.767	32.410	4.6	1.57	0.90	43.0	36.9
SF30	30	12.64	2.488	11.226	44.7	5.88	4.16	29.1	25.9
SF35	35	11.92	1.996	12.652	21.7	5.59	6.56	22.9	19.5
SF40	40	12.41	0.662	3.406	39.3	14.83	0.29	20.9	18.0

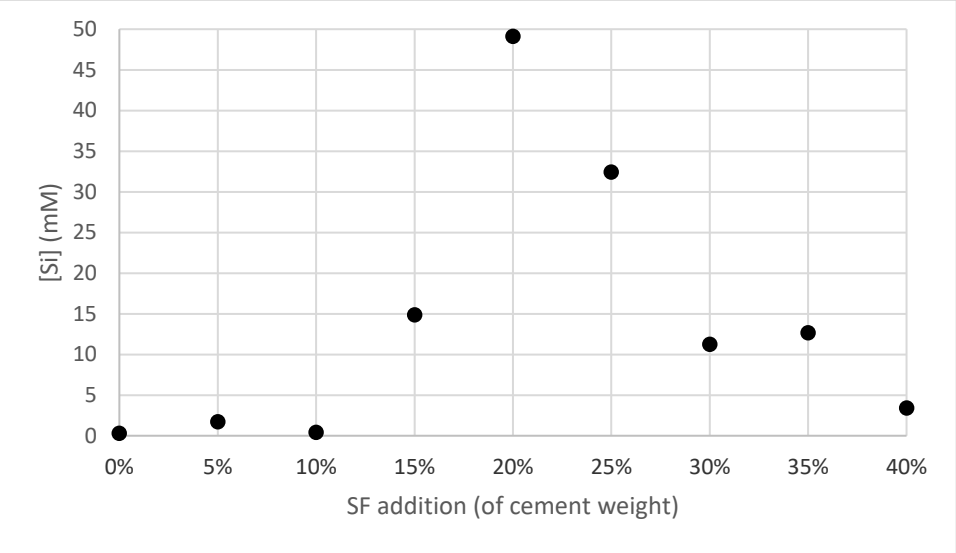

Figure 1. Silicate concentration vs. SF addition

3.2. Electrochemical analysis

The CV results are presented separately for solutions without a NaCl addition and for solutions with a NaCl addition.

3.2.1. CV in solutions without NaCl

A sample of CV graphs for 0, 0.356, 3.56, 35.6 mM silicate are presented in **Figure 2**.

Preprints (www.preprints.org) | NOT PEER-REVIEWED | Posted: 14 October 2020

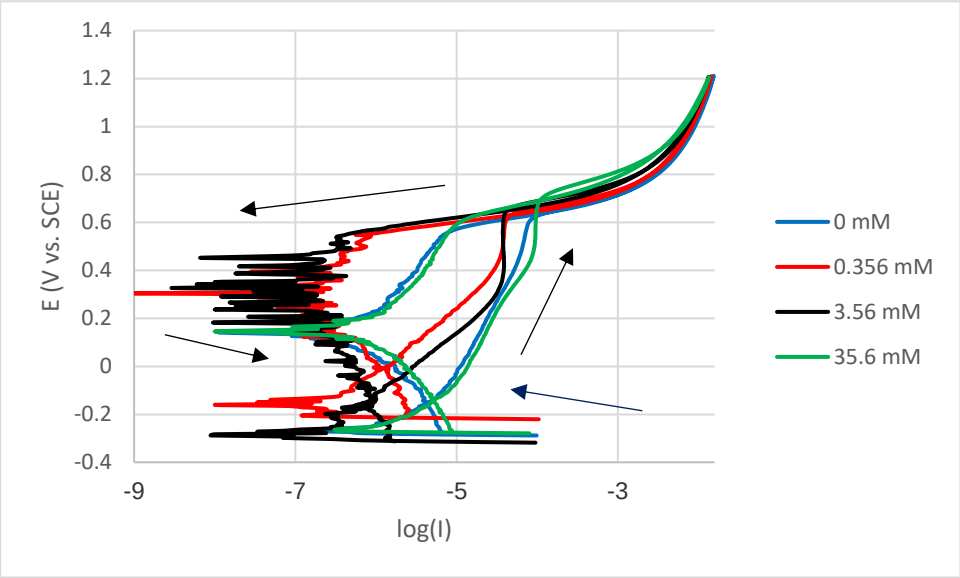

Figure 2. CV graph for reinforcing steel in 0 – 35.6 mM silicate , pH 13. Arrows show the direction of change

The OCP of steel which has not been exposed to chloride has a tendency to decrease with silicate concentration, but the variation for each silicate concentration is high (**Figure 3**).

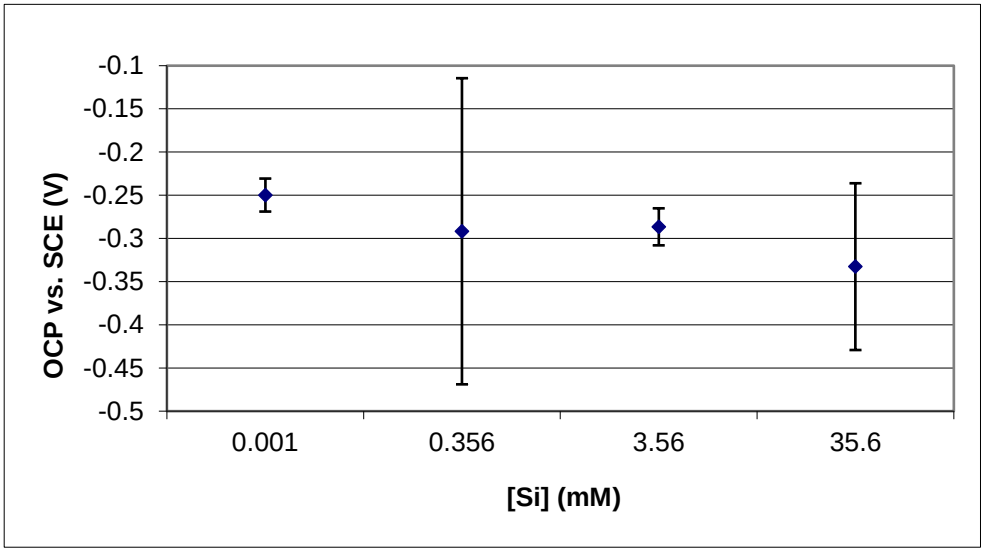

Figure 3. The undisturbed OCP for different silicate concentrations, before CV

The positive potential offset of the OCP during measurement increases from 0.33 V to 0.7 V as silicate concentration increases from 0 to 3.56 mM silicate, , and then decreases to 0.55 V for 35.6 mM silicate (Figure 4).

Preprints (www.preprints.org) | NOT PEER-REVIEWED | Posted: 14 October 2020

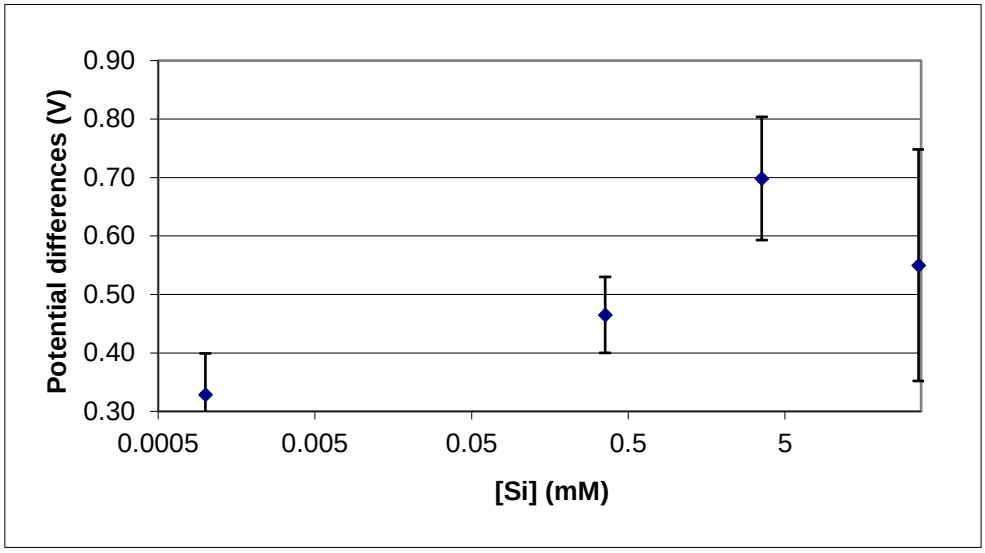

Figure 4. Positive difference of OCP from the undisturbed state to the OCP after CP, in different silicate solutions. 0 mM was entered as 10^{-3} mM to enable the logarithmic scale.

3.2.2. CV in solutions containing NaCl

For silicate concentrations up to 3.56 mM the OCP-before-CV is higher than the OCP-after-CV. For a concentration of 35.6 mM, the OCP-before-CV is lower than the OCP-after-CV (Figure 5). After CV, localized corrosion could be seen on the specimens' surface with a silicate concentration of 0 to 3.56 mM (Figure 6). No corrosion sign could be seen on the 35.6 mM specimen.

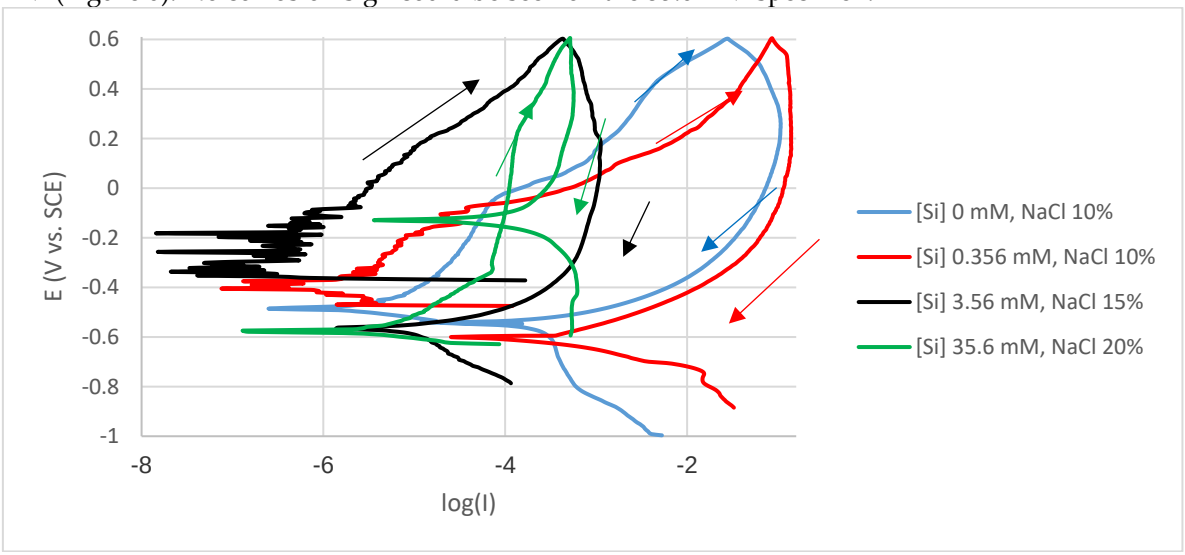

Figure 5. CV graphs for different silicate concentrations in NaCl solutions. Arrows show the direction of change.

Preprints (www.preprints.org) | NOT PEER-REVIEWED | Posted: 14 October 2020

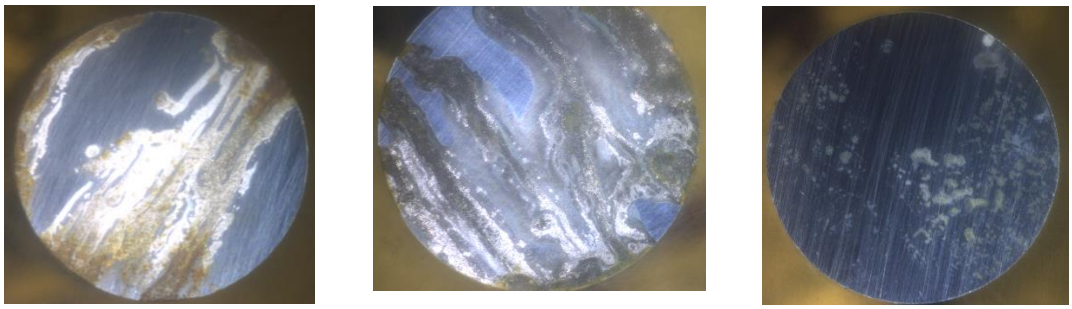

(a) (b) (c)

Figure 6. Specimens after CV in NaCl solutions. (a) 0 mM silicate, 10% NaCl (b) 0.356 mM silicate, 10% NaCl (c) 3.56 mM silicate, 15% NaCl

The OCP and corrosion current density, before and after CV, of 35.6 mM silicate specimens in different NaCl solutions are shown in **Table 7** and Figure 7. Current density for silicate concentration of 35.6 mM vs. NaCl concentration at the start and end of CV. The corrosion current density rises with NaCl concentration. Except for the measurement without NaCl, the current after CV is higher than the current before CV.

Table 7. OCP (V vs. SCE), and corrosion current density, i (Acm^{-2}), for silicate concentration of 35.6 mM and varied NaCl concentrations. Subscript s – start of CV, e – end of CV.

% NaCl	0	10	15	20
OCP_s	-0.264	-0.532	-0.502	-0.574
OCP_e	0.191	-0.107	-0.107	-0.129
i_s	3.04E-07	4.63E-07	1.57E-06	2.32E-06
i_e	6.88E-08	2.42E-06	5.64E-06	3.84E-05

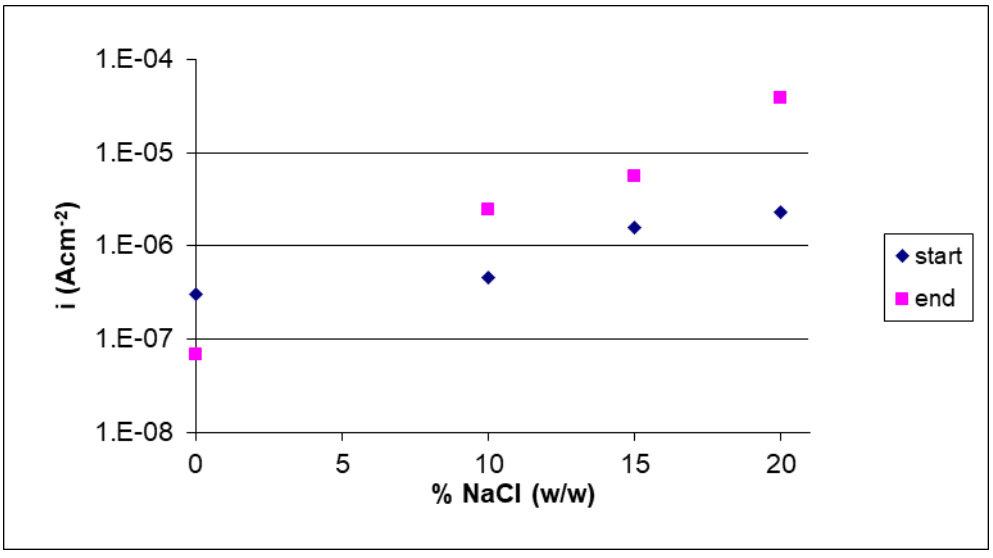

Figure 7. Current density for silicate concentration of 35.6 mM vs. NaCl concentration at the start and end of CV

The electrochemical parameters which can be extracted from the CV graph analysis, the OCP potential of passive and corroding specimens, and current at the passive state and at pit initiation, are shown in **Table 8** with a calculation of the current density at the active state, passive state, and pit initiation.

Table 8. Electrochemical parameters for different silicate concentrations.

Preprints (www.preprints.org) | NOT PEER-REVIEWED | Posted: 14 October 2020

Parameter	units	0 mM	0.356 mM	3.56 mM
E_{ocp}	V vs SCE	-0.486	-0.405	-0.337
$I_{passive}$	A	1.26E-06	3.84E-08	3.12E-16
$I_{pit\text{-}initiation}$	A	1.18E-03	1.23E-02	4.68E-04
Total area	cm^2	0.785	0.785	0.785
Corroded area	cm^2	0.536	0.725	0.169
E_{cor}	V vs SCE	-0.541	-0.600	-0.567
I_{act}	A	1.06E-04	2.01E-04	3.44E-06
i_{act}	Acm^{-2}	1.97E-04	2.78E-04	2.03E-05
$i_{passive}$	Acm^{-2}	1.60E-06	4.89E-08	3.97E-16
$i_{pit\text{-}initiation}$	Acm^{-2}	2.19E-03	1.70E-02	2.77E-03

4. Discussion

4.1. Pore solution

Up to a 10% addition of SF, the silicate concentration found in this work was in the range which can be found in the literature for ordinary Portland cement, white Portland cement, and its blends with limestone powder and slug [41], [43]–[47], [62], which is usually below 0.5 mM, or up to 1.5 mM in cement containing fly-ash [47]. It is clear that an increase of the SF content above 10% of cement content is associated with an increase of soluble silicate (**Figure 1**). It seems that a maximum concentration is achieved with an addition of 15% to 25% SF; while of the compositions studied in this work, 20% SF yielded the maximum concentration of 49 mM. These concentrations of SF are much higher than the concentrations in current practice which are limited by experience and standards to 10% of total binder. However, the SF in this work does serve as a model material for pozzolans. Other pozzolans are introduced in concrete mixes and blended cements in higher contents. The European norm for cement, EN 197 – 2011, permits up to 35% pozzelanic content in CEM II/B, and up to 55% in CEM IV/B. This is without taking GGBS in account, which can be up to 95% in CEM III/C. The silica content in the pozzolanic materials can be higher than 50%, thus providing sufficient silica to the mix.

The solubility of the silica in pozzolan is a field not well studied. Assuming that the system is at equilibrium after 3 months, a solubility constant (K_{sp}) can be calculated to predict system equilibria for other pozzolans. The data in this work is not sufficient for accurate calculation of K_{sp}. As a reference for future studies, the calculated K_{sp}s are supplied in Appendix B.

4.2.Electrochemical analysis

The CV technique was found to be the most appropriate for this study. However, other techniques were examined as well. These yield data and insights which may be of use in future research, and we include them in Appendix C.

4.2.1. CV in solutions without NaCl

The second peak, i.e. the peak after forcing galvanic corrosion, OCP_e, has a higher OCP than the OCP before CV initiation (**Figure 2**). This implies that pitting has not been initiated, and that passivation was strengthened by the induced current. For silicate concentrations of 0.356 and 3.56 mM silicate, the new OCP corrosion current is so low that the measured signal is noisy, due to currents below 10^{-7} Ampere.

The OCP of the specimens before CV (OCP_i) shows a slight decrease as silicate concentration increases (**Figure 3**). High variation in results make this tendency insignificant. On the other hand, since EP is often used as indicator for the state of reinforcement corrosion, this variation draws attention to the limitation of EP as a corrosion indicator.

The difference between after-CV-OCP (OCP_e) and before-CV-OCP (OCP_i) increases with silicate concentrations up to 3.56 mM silicate. The potential difference for the 35.6 mM silicate solution is also higher than the 0 mM silicate solution (**Figure 4**). This finding, along with the decrease in the

Preprints (www.preprints.org) | NOT PEER-REVIEWED | Posted: 14 October 2020

corrosion current at the OCP, indicates that soluble silicate improves the properties of the passive layer. The question is, how does it improve the layer in the case of chloride-induced corrosion. It is known that corrosion of reinforcements does initiate due to exposure to chloride, and that this corrosion initiates with pitting. In this experiment, no pitting was observed. Hence, a CV study with chloride is needed.

4.2.2. CV in solutions containing NaCl

Reviewing the relation between chloride concentration in solution and the corrosion current at the passive state: for a silicate concentration of 35.6 mM (**Table 7** and **Figure 7**) the current was seen to increase with increasing chloride concentrations. This result supports the theoretical explanation for chloride-induced corrosion initiation in concrete. The current rises with the chloride concentration, until the factor of the current density multiplied by the local pit depth ($i \cdot x$) is high enough to create a concentration polarization, which produces a pH at the bottom of the groove that is low enough for the passivation layer breakdown [63]–[65]. The higher stability of silica at a low pH may explain the better pitting resistance of steel in high silicate-containing solutions. This theory also explains the lower chloride threshold found for specimens with rough surfaces, relative to those with smooth surfaces [37], [66]–[68].

For models of corrosion initiation, the information about current density at pit initiation, $i_{pit\text{-}initiation}$, may be valuable. The pit initiation corrosion current is in the range of 1.70E-2 to 2.19E-3 Acm^{-2}. This current is one order of magnitude higher than reported in [61], which is 6.9E-4 Acm^{-2}, but similar to those in the references cited in [61]. This can be explained by the polished surface. Since the corrosion current for pitting initiation depends on the initial roughness of the surface, a polished surface has shallower defects. This results in higher currents for pit initiation. Small defects on a polished surface can have a higher variation in their relative depths, which can influence the corrosion current for pit initiation more than other factors, and be a significant source for deviation in results especially when characteristics of corrosion initiation, such as pit initiation current, are investigated. For more accurate results in a future study, creating pits of known dimensions prior to the electrochemical tests will make any small uncontrollable roughness negligible.

The passive corrosion current density, $i_{passive}$, (**Table 7.** OCP (V vs. SCE), and corrosion current density, i (Acm^{-2}), for silicate concentration of 35.6 mM and varied NaCl concentrations. Subscript s – start of CV, e – end of CV. and **Table 8.** Electrochemical parameters for different silicate concentrations.) decreases with silicate concentrations from 0 to 3.56 mM, but the 35.6 mM specimen demonstrates a passive current density similar to that of the 0 mM; and for an NaCl concentration of 20% the passive corrosion current is similar to the active corrosion current of the 3.56 mM silicate concentration. This result is in contrast to what might be expected. According to Oliveira et al. [51] the corrosion currents obtained in a silicate solution of 1 M as Si are in the range of 10^{-6}-10^{-7} Acm^{-2} (excluding cathodic treatment which is irrelevant). These results are in the same range as those found in this work, but in a different environment. Nevertheless, with a higher silicate concentration the passive corrosion current wasn't lower than the passive current in this study, and the corrosion current of the 3.56 mM silicate was much lower. This hints that an optimal silicate concentration for inhibition of corrosion may indeed exist.

5. Conclusions

In this study the pore solution compositions of cement pastes having different SF contents was measured. An analysis was made of the electrochemical behavior of reinforcing steel in silicate solutions at the range typically found in pore solutions. The main findings are:

- Silicate (i.e. dissolved silica) concentrations in a concrete pore solution may vary by up to three orders of magnitude, due to the use of pozzolans.
- Cyclic voltammetry was found to be an adequate method for the investigation of corrosion inhibition resulting from the chemical composition of pore solutions. This technique gives

Preprints (www.preprints.org) | NOT PEER-REVIEWED | Posted: 14 October 2020

results which are in agreement with those that have been found for localized chloride-induced corrosion initiation.

- There is clear evidence that an increase of soluble silicate, at least up to 3.56 mM, increases the resistance of steel to chloride-induced pit initiation. This implies that a pozzolan content equivalent to 15% SF or more may increase RC resistance to chloride-induced corrosion.
- Reducing surface variability by creating controlled pit depths is advised for further research regarding corrosion initiation in simulated pore solutions.

Supplementary Materials:

Author Contributions: Conceptualization, A. Kenny and A. Katz; methodology, A. Kenny; software, A. Kenny; validation, A. Kenny; formal analysis, A. Kenny; investigation, A. Kenny; resources, A. Katz; data curation, A. Kenny; writing—original draft preparation, A. Kenny; writing—review and editing, A. Kenny and A. Katz; visualization, A. Kenny; supervision, A. Katz; project administration, A. Katz; funding acquisition, A. Katz; All authors have read and agreed to the published version of the manuscript.

Funding: This research was funded by MINISTRY OF CONSTRUCTION AND HOUSING OF ISRAEL, grant number 4500386280.

Acknowledgments: the authors acknowledge the help and support in the form of lab work and use of laboratory equipment of Prof. Avraham Shaviv laboratory in the faculty of Civil end Environmental Eng. and Prof. Yair Ein-Eli laboratory in the Department of Material Science and Engineering, both at the Technion – IIT.

Conflicts of Interest: The authors declare no conflict of interest.

Appendix A

A.1. Validation of pore solution chemical analysis method

Because the volume of extracted pore solution is often less than 2 ml, pore solution drops were collected by syringe, and diluted. This process may introduce error into the measurement in two ways: (a) carbonation, which reduces pH; and (b) deviation of the calculated pH due to the pk_b of the species in the solution. To assess the deviation, small synthetic pore solution drops were spread on the extraction device base. The drops were collected by syringe, filtered and diluted, as in the method for pore solution analysis; and their pH was measured.

The results show a maximum change of -0.22 pH units, while the deviation during 5-25 minutes, which is the common time for extraction and sample collection, is less than 0.1 pH unit (**Table**). This deviation should be taken into account when using the Ksp in Appendix B.

Table A.1 Time from spread, calculated pH, and deviation of the pH from the original value

Time from spread	Calculated pH	Deviation
0	13.17	0.14
5	13.10	0.07
10	13.08	0.05
15	13.07	0.04
20	13.03	0.01
25	13.00	-0.02
30	12.80	-0.22
35	12.88	-0.14

A.2. Comparison with dissolution from solids

Because the extraction procedure is expensive, the results were compared to the results achieved by pulverizing a sample and extracting via deionized water as described by Behnood et al. as ex-situ leaching method [69]. The specimen which was used was 5% SF. It is clear that extraction by pulverization and water addition is dominated by calcium hydroxide dissolution. The results show

Preprints (www.preprints.org) | NOT PEER-REVIEWED | Posted: 14 October 2020

that pulverized concrete extraction by water is inadequate for pore solution analysis (**Table** and **Table**).

Table A.2. Pore solution pH by different extraction methods of 5% SF mix

Method	pH
As described in 2.2, 2.3	13.13
Pulverized concrete after 2 hours agitation	12.78
Pulverized concrete after 2 days agitation	12.80

Table A.3. Chemical composition of solution by different extraction methods of 5% SF mix

Method	Ca	Si	Al	Fe	Mg	K	Na
As described in 2.2, 2.3	48.8	48.31	0.50	0.05	0	2626	1638
Pulverized concrete after 2 days agitation	506.1	0.853	0.11	0.004	0	532	292

Appendix B

The solubility constant, Ksp, can be theoretically calculated from the logarithm of the concentrations. Deviation from the equilibrium and any error in calculated pH may introduce errors into this calculation. Because the equilibrium involves many ion species, and some ions such assulfate are not being measured, there is a need for at least 80 independent measurements of concentration. However, any contribution to the data about hydrated cement solubility is important, because such data is scarce. Hence, the calculation of the solubility constant is presented in this appendix.

The calculation is performed on the negative logarithm of concentrations and the constant, known as "p"[1], by using linear regression. Ions of metals of minor importance, Al, Fe, and Mg were omitted, to reduce overfitting. The p`s values are shown in **Table** . The result of the regression is:

$$pk_{sp} = 2.67 \cdot pCa + 8.20 \cdot pK - 6.87 \cdot pNa - 0.51 \cdot pSi + pH = 21.13, \quad (1)$$

The standard deviation of the Ksp of the different samples is 2.56%, which is equivalent to 0.54 in pKsp units.

Table B.1 The negative logarithm, "p" of the ions measured in the extraction

Notation	pH	pCa	pSi	pK	pNa
SF0	13.55	3.46	3.53	0.75	0.87
SF5	13.13	2.91	2.76	1.17	1.14
SF10	12.86	2.82	3.38	1.46	1.42
SF15	11.44	3.03	1.82	1.49	1.44
SF20	12.50	2.84	1.30	1.37	1.34
SF25	11.76	3.11	1.48	1.36	1.43
SF30	12.64	2.60	1.94	1.53	1.58
SF35	11.92	2.70	1.89	1.63	1.71
SF40	12.41	3.18	2.46	1.68	1.74
SF5 by pulverization	12.8	1.90	4.51	1.87	1.89

Ions with an equal sign in equation (1) are competitive, i.e. when one increases the other decreases. Thus, Ca and K are competitive, and pH, Si and Na are competitive. It makes sense that ions with the same sign will solute one at the expense of the other, as do Ca and K, and Si and pH. However, the inclusion of Na with the Si and pH does not make sense. The Na could be expected to compete with

[1] For example pKsp=-log$_{10}$(Ksp)

Preprints (www.preprints.org) | NOT PEER-REVIEWED | Posted: 14 October 2020

K, but as can be seen, the ratio K/Na is fixed (**Table 6**), so it may be an artifact arising from the small differences between K and Na. In any case, this topic deserve separate study.

Entering to equation (1) the concentrations data for the extraction by pulverization and water addition yield 17.87, very far from 21.13, more than 6 standard deviation. It can be conclude that the method of extraction by pulverization and water addition has no value in the study of concrete pore solution.

Appendix C

Other electrochemical methods were used during this study, and are not reported in the main text. A comparison between these methods is reported here to explain why the method chosen for this study is the most appropriate one.

C.1. EP vs. time

Specimens were fabricated first without immersion in silicate solution prior to the epoxy cast. The corrosion in all these specimens had started as crevice corrosion between the steel and the epoxy. The results were completely random. It seems that surface microscopic defects had more influence on results than silicate and chloride concentrations. The EP vs. time of specimens, as described in the method section, (Figure C.1.) tends to rise in the first 14 days. An addition of 3% NaCl at the 57th day caused a temporary reduction of the EP, which rose to approximately its former value after one to several days. Raising the NaCl concentration to 4% gave similar results. Measuring the EP change after NaCl addition yielded no clear results (Figure C.2.). It may be concluded that these experiments contained no valuable information regarding the effect of silicate concentration on chloride-induced corrosion inhibition.

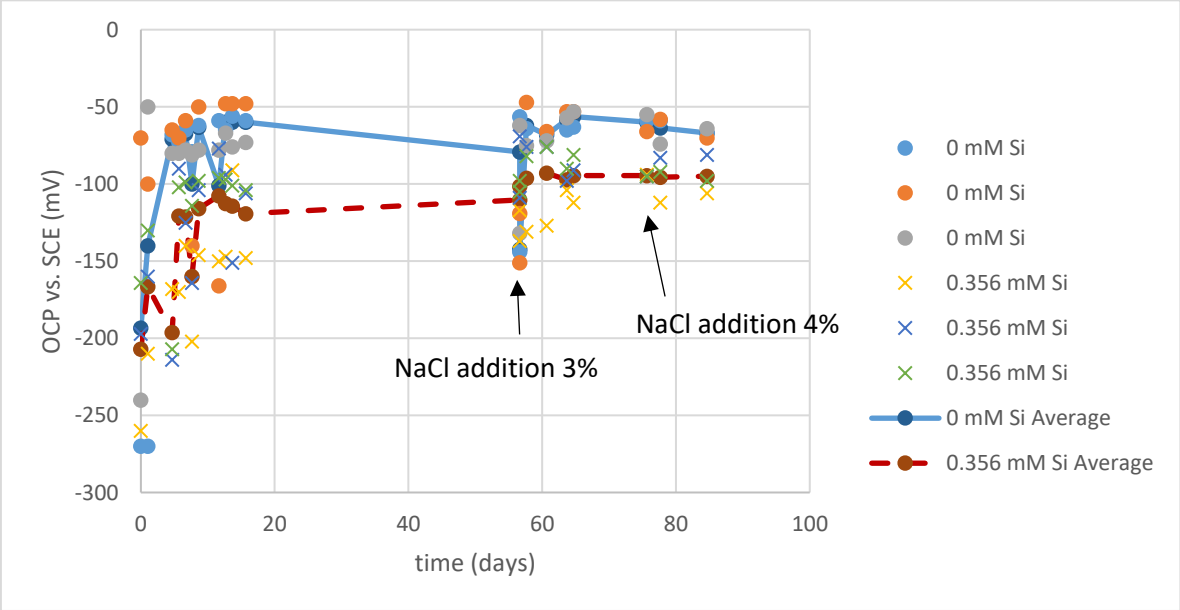

Figure C.1. OCP vs. time for specimens in different solutions

Preprints (www.preprints.org) | NOT PEER-REVIEWED | Posted: 14 October 2020

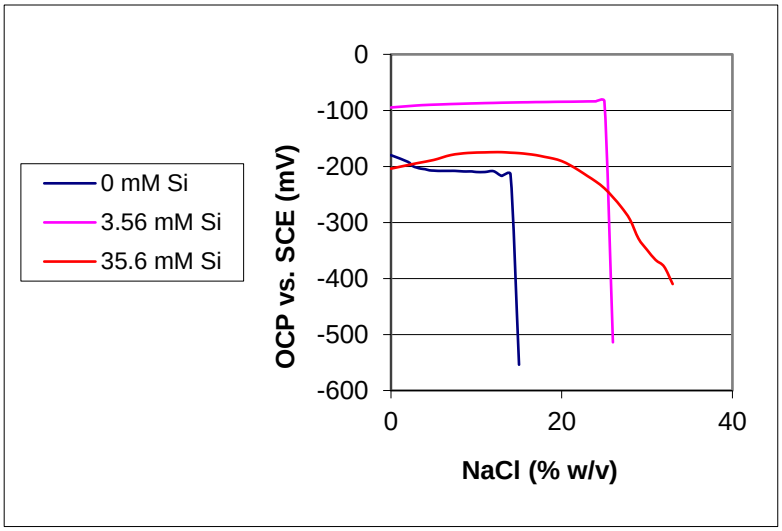

Figure C.2. OCP vs. chloride concentration

C.2. EIS (Rp)

The use of EIS gives a reliable measurement of the Rp. Since the corrosion current can be determined by CV, the EIS was used only during the preliminary study. Spectra demonstrated two time constants. In any case, no difference was found in the quality of curve fitting to Rs,Rp||CPE,R2||C2 or Rs,Rp||CPE circuits (Figure C.3.), nor in the resulting Rp.

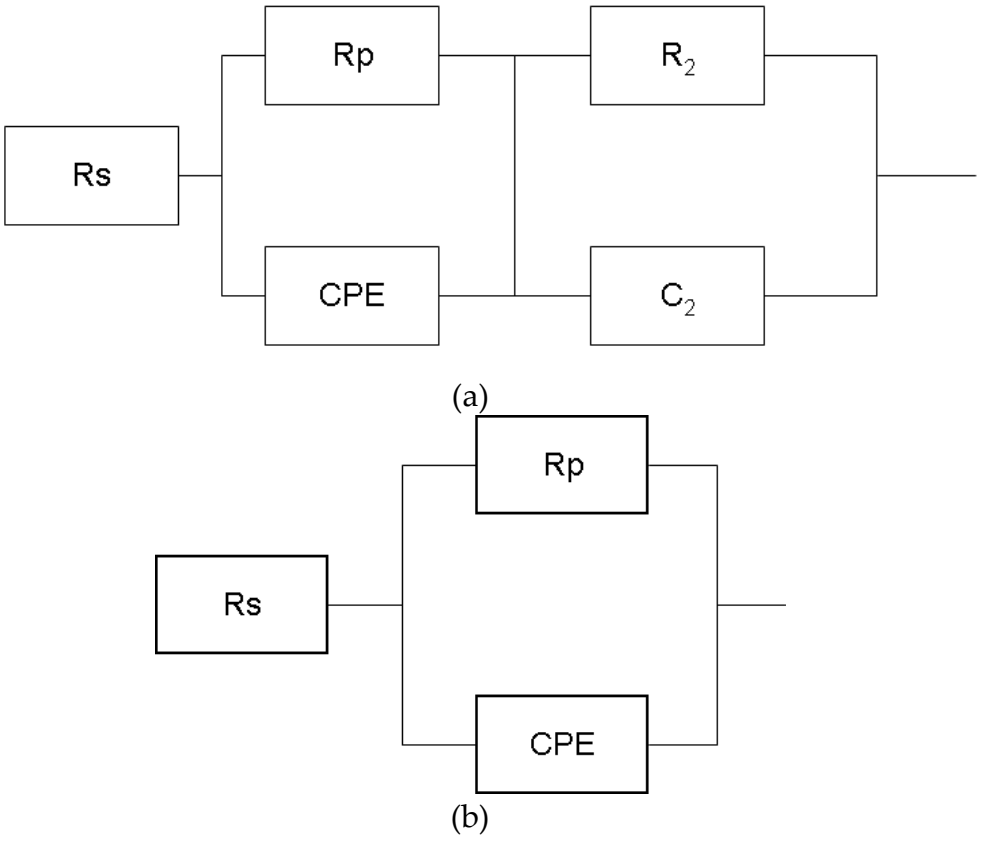

Figure C.3. Equivalent circuits. (a) Rs,Rp||CPE,R_2||C_2, (b) Rs,Rp||CPE

There was no significant change of Rp with time after more than one day following immersion. However, there is a clear segregation into two groups: Rp in the range of 1E6 Ω and Rp in the range of 1E14 Ω. In the latter group, only specimens immersed in silicate solution can be found (Figure

Preprints (www.preprints.org) | NOT PEER-REVIEWED | Posted: 14 October 2020

and **Figure 8**). As long as the specimen is not corroding, the chloride concentrations do not affect this segregation. When graphing the OCP vs. Rp, the points settle on two separated lines (**Figure 8**). The two lines correspond well with those found for the measurement of steel in concrete, reported in [70] (**Figure 8**, green dots). This hints that in the presence of silicate, two different types of passive layer may be formed. Due to the limited scope of this study, this subject has not been further investigated.

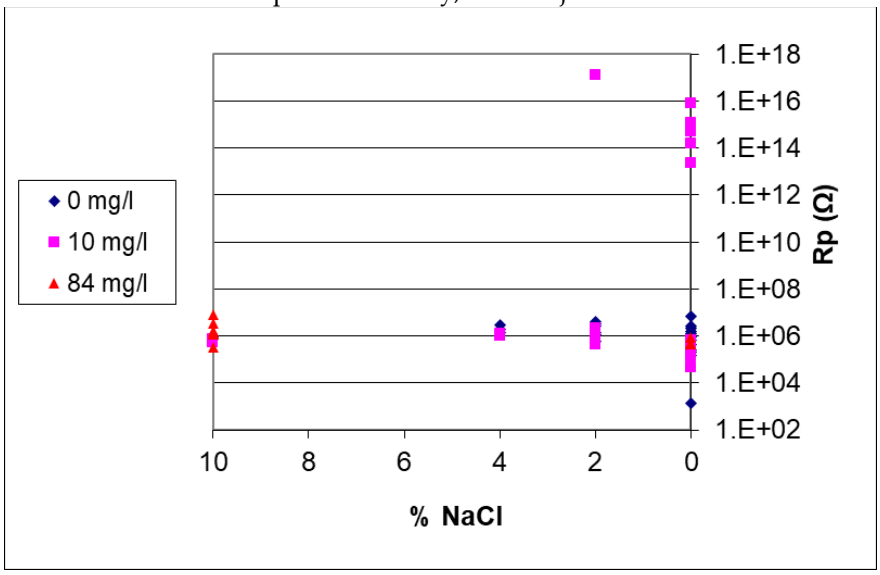

Figure C.4. Rp measured for three different silicate concentrations (as Si), in different NaCl concentrations

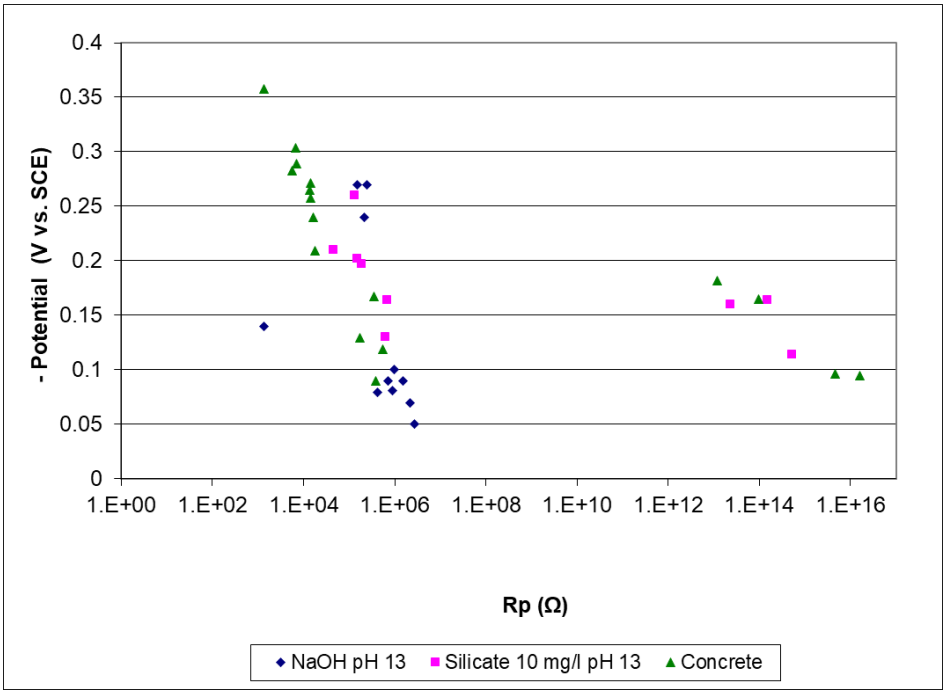

Figure 8.5. –EP vs. Rp for specimens in NaOH pH 13 solution, 10 mg/l (as Si) silicat pH 13 solution, and steel embedded in concrete from [70]

References

[1] U. M. Angst, "Challenges and opportunities in corrosion of steel in concrete," *Mater. Struct. Constr.*, vol. 51, no. 1, 2018, doi: 10.1617/s11527-017-1131-6.

[2] G. H. Koch, M. P. H. Brongers, N. G. Thompson, Y. P. Virmani, and J. H. Payer, "Corrosion Cost and Preventive Strategies in the United States," http://www.corrosioncost.com/pdf/main.pdf, 2001.

Preprints (www.preprints.org) | NOT PEER-REVIEWED | Posted: 14 October 2020

[3] M. Kawamura, D. Singhal, and Y. Tsuji, "Effects of interfacial transition zone around reinforcement on its corrosion in mortars with and without a reactive aggregate," in *Proceeding of the international RILEM conference No. 35 The interfacial zone in cementitious composites*, 1998, pp. 179 {----} 186.

[4] T. U. Mohammed and H. Hamada, "A discussion of the paper 'Chloride threshold values to depassivate reinforcing bars embedded in a standardized OPC mortar' by C. Alonso, C. Andrade, M. Castellote, and P. Castro," *Cem. Concr. Res.*, vol. 31, no. 5, pp. 835–838, 2001, doi: 10.1016/S0008-8846(01)00485-9.

[5] I. G. Ogunsanya, V. Strong, and C. M. Hansson, "Corrosion behavior of austenitic 304L and 316LN stainless steel clad reinforcing bars in cracked concrete," *Mater. Corros.*, vol. 71, no. 7, pp. 1066–1080, 2020, doi: 10.1002/maco.201911221.

[6] R. G. Duarte, A. S. Castela, R. Neves, L. Freire, and M. F. Montemor, "Corrosion behavior of stainless steel rebars embedded in concrete: An electrochemical impedance spectroscopy study," *Electrochim. Acta*, vol. 124, pp. 218–224, 2014, doi: 10.1016/j.electacta.2013.11.154.

[7] B. H. Oh, S. Y. Jang, and Y. S. Shin, "Experimental investigation of the threshold chloride concentration for corrosion initiation in reinforced concrete structures," *Mag. Concr. Res.*, vol. 55, no. 2, pp. 117–124, 2003.

[8] M. Thomas, "Chloride thresholds in marine concrete," *Cem. Concr. Res.*, vol. 26, no. 4, pp. 513–519, 1996.

[9] O. A. Kayyali and M. N. Haque, "The ratio of Cl$-$/OH$-$ in chloride contaminated concrete. A most important criterion," *Mag. Concr. Res.*, vol. 47, pp. 235{----}242, 1995.

[10] P. Schiessl and W. Breit, "Local repair measures at concrete structures damaged by reinforcement corrosion," in *Proceedings of the Fourth International Symposium on Corrosion of Reinforcement in Concrete Construction, SCI, Cambridge*, 1996, pp. 525{----}534.

[11] P. B. Bamforth, "The derivation of input data for modelling chloride ingress from eight{}-years UK coastal exposure trials," *Mag. Concr. Res.*, vol. 51, pp. 87–96, 1999.

[12] P. Lambert, C. L. Page, and P. R. W. Vassie, "Investigation of reinforcement corrosion. Electrochemical monitoring of steel in chloride contaminated concrete," *Mater. Struct.*, vol. 24, pp. 351{----}358, 1991.

[13] B. B. Hope and A. K. C. Ip, "Corrosion inhibitors for use in concrete," *ACI Mater. J.*, vol. 86, no. 6, pp. 602–608, 1989.

[14] K. H. Pettersson, *Factors influencing chloride induced corrosion of reinforcement in concrete*, vol. 1. Chapman & Hall, London, 1996.

[15] Pettersson, "Chloride threshold value and the corrosion rate in reinforced concrete," in *Proceedings of the International Conference on Corrosion and Protection of Steel in Concrete*, 1994, p. 461.

[16] K. Petterson, "Corrosion threshold value and corrosion rate in reinforced concrete," 1992.

[17] S. E. Hussain, Rasheeduzzafar, A. Al-Musallam, and A. S. Al-Gahtani, "Factors affecting threshold chloride for reinforcement corrosion in concrete," *Cem. Concr. Res.*, vol. 25, no. 7, pp. 1543–1555, 1995.

[18] P. Schiessl and M. Raupach, "Influence of concrete composition and microclimate on the critical chloride content in concrete.," in *Proceedings of the Third International Symposium On Corrosion of Reinforcement in Concrete*, 1990, p. 49.

[19] K. W. J. Treadaway, B. L. Brown, and R. N. Cox, "Durability of corrosion resisting steels in concrete," in *Proceeding of Institution of Civil Engineers*, 1989, pp. 305–331.

[20] V. K. Gouda and W. Y. Halaka, "Corrosion and corrosion inhibition of reinforced steel," *Br. Corros. J.*, vol. 5, pp. 204{----}208, 1970.

[21] G. K. Glass and B. Reddy, "The Influence of the Steel Concrete Interface on the Risk of Chloride Induced Corrosion Initiation," in *COST 521, Final Workshop, Luxembourgh, 18{}-19 February 2002*, 2002, p. S. 227--232.

Preprints (www.preprints.org) | NOT PEER-REVIEWED | Posted: 14 October 2020

[22] H. Nahali, L. Dhouibi, and H. Idrissi, "Effect of Na3PO4 addition in mortar on steel reinforcement corrosion behavior in 3% NaCl solution," *Constr. Build. Mater.*, vol. 78, pp. 92–101, 2015, doi: 10.1016/j.conbuildmat.2014.12.099.

[23] W. Breit and P. Schiesl, "Investigation on the threshold value of the critical chloride content," in *Proceeding of the 4th CANMET/ACI international conference on durability of concrete*, 1997, vol. 1, pp. 363–378.

[24] C. Alonso, M. Castellote, and C. Andrade, "Chloride threshold dependence of pitting potential of reinforcements," *Electrochim. Acta*, vol. 47, no. 21, pp. 3469–3481, 2002.

[25] C. Andrade and C. L. Page, "Pore solution chemistry and corrosion in hydrated cement systems containing chloride salts. A study of cation specific effects," *Cem. Concr. Res.*, vol. 21, no. 1, pp. 49–53, 1986.

[26] H. Luo, H. Su, C. Dong, and X. Li, "Passivation and electrochemical behavior of 316L stainless steel in chlorinated simulated concrete pore solution," *Appl. Surf. Sci.*, vol. 400, pp. 38–48, 2017, doi: 10.1016/j.apsusc.2016.12.180.

[27] Y. qi Wang, G. Kong, C. shan Che, and B. Zhang, "Inhibitive effect of sodium molybdate on the corrosion behavior of galvanized steel in simulated concrete pore solution," *Constr. Build. Mater.*, vol. 162, pp. 383–392, 2018, doi: 10.1016/j.conbuildmat.2017.12.035.

[28] Z. Ai *et al.*, "Passive behaviour of alloy corrosion-resistant steel Cr10Mo1 in simulating concrete pore solutions with different pH," *Appl. Surf. Sci.*, vol. 389, pp. 1126–1136, 2016, doi: 10.1016/j.apsusc.2016.07.142.

[29] A. Królikowski and J. Kuziak, "Impedance study on calcium nitrite as a penetrating corrosion inhibitor for steel in concrete," in *Electrochimica Acta*, 2011, vol. 56, no. 23, pp. 7845–7853, doi: 10.1016/j.electacta.2011.01.069.

[30] V. K. Gouda, "Corrosion and corrosion inhibition of reinforcing steel; 1 {--} Immersion in alkaline solution," *Br. Corros. J.*, vol. 5, pp. 198{----}203, 1970.

[31] S. Goñi and C. Andrade, "Synthetic concrete pore solution chemistry and rebar corrosion rate in the presence of chlorides," *Cem. Concr. Res.*, vol. 20, pp. 525–539, 1990.

[32] D. Izquierdo, C. Alonso, C. Andrade, and M. Castellote, "Potentiostatic determination of chloride threshold values for rebar depassivation experimental and statistical study," *Electrochim. Acta*, vol. 49, no. 17–18, pp. 2731–2739, 2004.

[33] J. Nam, W. H. Hartt, and K. Kim, "Time to corrosion of reinforcing steel in concrete specimens as affected by alkalinity and bar surface condition," in *Corrosion 2005*, 2005, p. paper # 05256.

[34] A. Aldykiewicz, N. S. Berke, R. J. Hoops, and L. Li, "Long-term behavior of fly ash and silica fume concretes in laboratory and field exposures to chlorides," 2005.

[35] K. M. A. Hossain, "Chloride induced corrosion of reinforcement in volcanic ash and pumice based blended concrete," *Cem. Concr. Compos.*, vol. 27, pp. 381–390, 2005.

[36] A. Kenny and A. Katz, "A Statistical Analysis of the Distribution of the Chloride Threshold with Relation to Steel-concrete Interface," *Am. J. Constr. Build. Mater.*, vol. 3, no. 1, p. 16, 2019, doi: 10.11648/j.ajcbm.20190301.13.

[37] U. M. Angst *et al.*, "The effect of the steel--concrete interface on chloride-induced corrosion initiation in concrete: a critical review by RILEM TC 262-SCI," *Mater. Struct.*, vol. 52, no. 4, p. 88, 2019, doi: 10.1617/s11527-019-1387-0.

[38] A. Kenny and A. Katz, "Statistical relationship between mix properties and the interfacial transition zone around embedded rebar," *Cem. Concr. Compos.*, vol. 60, 2015, doi: 10.1016/j.cemconcomp.2015.04.002.

Preprints (www.preprints.org) | NOT PEER-REVIEWED | Posted: 14 October 2020

[39] L. Li and A. A. Sagüés, "Chloride corrosion threshold of reinforcing steel in alkaline solutions {}- open{}-circuit imersion tests," *Corrosion*, vol. 57, no. 1, pp. 19{}--28, 2001.

[40] L. Li and A. A. Sagues, "Chloride threshold of reinforcing steel in alkaline solutions{}-effect of specimen size," *Corrosion*, vol. 60, no. 2, pp. 195–202, 2004.

[41] D. Rothstein, J. J. Thomas, B. J. Christensen, and H. M. Jennings, "Solubility behavior of Ca-, S-, Al-, and Si-bearing solid phases in Portland cement pore solutions as a function of hydration time," *Cem. Concr. Res.*, vol. 32, no. 10, pp. 1663–1671, 2002, doi: DOI: 10.1016/S0008-8846(02)00855-4.

[42] S. Song and H. M. Jennings, "Pore solution chemistry of alkali-activated ground granulated blast-furnace slag," *Cem. Concr. Res.*, vol. 29, no. 2, pp. 159–170, 1999, doi: 10.1016/S0008-8846(98)00212-9.

[43] B. Lothenbach, G. Le Saout, E. Gallucci, and K. Scrivener, "Influence of limestone on the hydration of Portland cements," *Cem. Concr. Res.*, vol. 38, no. 6, pp. 848–860, Jun. 2008, doi: 10.1016/j.cemconres.2008.01.002.

[44] K. De Weerdt, M. Ben Haha, G. Le Saout, K. O. Kjellsen, H. Justnes, and B. Lothenbach, "Hydration mechanisms of ternary Portland cements containing limestone powder and fly ash," *Cem. Concr. Res.*, vol. 41, no. 3, pp. 279–291, Mar. 2011, doi: 10.1016/j.cemconres.2010.11.014.

[45] S. Adu-Amankwah, M. Zajac, C. Stabler, B. Lothenbach, and L. Black, "Influence of limestone on the hydration of ternary slag cements," *Cem. Concr. Res.*, vol. 100, pp. 96–109, Oct. 2017, doi: 10.1016/j.cemconres.2017.05.013.

[46] M. Zajac, J. Skocek, B. Lothenbach, and B. H. Mohsen, "Late hydration kinetics: Indications from thermodynamic analysis of pore solution data," *Cem. Concr. Res.*, vol. 129, p. 105975, Mar. 2020, doi: 10.1016/j.cemconres.2020.105975.

[47] F. Deschner, B. Lothenbach, F. Winnefeld, and J. Neubauer, "Effect of temperature on the hydration of Portland cement blended with siliceous fly ash," *Cem. Concr. Res.*, vol. 52, pp. 169–181, Oct. 2013, doi: 10.1016/j.cemconres.2013.07.006.

[48] F. Lollini, E. Redaelli, and L. Bertolini, "Investigation on the effect of supplementary cementitious materials on the critical chloride threshold of steel in concrete," *Mater. Struct. Constr.*, vol. 49, no. 10, pp. 4147–4165, 2016, doi: 10.1617/s11527-015-0778-0.

[49] C. Chalhoub, R. François, and M. Carcasses, "Critical chloride threshold values as a function of cement type and steel surface condition," *Cem. Concr. Res.*, vol. 134, p. 106086, 2020, doi: 10.1016/j.cemconres.2020.106086.

[50] N. Jordan, N. Marmier, C. Lomenech, E. Giffaut, and J. J. Ehrhardt, "Sorption of silicates on goethite, hematite, and magnetite: Experiments and modelling," *J. Colloid Interface Sci.*, vol. 312, no. 2, pp. 224–229, Aug. 2007, doi: 10.1016/j.jcis.2007.03.053.

[51] L. A. de Oliveira, O. V. Correa, D. J. dos Santos, A. A. Z. Páez, M. C. L. de Oliveira, and R. A. Antunes, "Effect of silicate-based films on the corrosion behavior of the API 5L X80 pipeline steel," *Corros. Sci.*, vol. 139, pp. 21–34, Jul. 2018, doi: 10.1016/j.corsci.2018.04.035.

[52] S. T. Amaral and I. L. Muller, "Effect of silicate on passive Films anodically formed on iron in alkaline solution as studied by Electrochimical Impedance Spectroscopy," *Corrosion*, vol. 55, no. 1, pp. 17–23, 1999.

[53] S. T. Amaral and I. L. Müller, "A RRDE study of the electrochemical behavior of iron in solutions containing silicate and sulphate at pH 10{}-13," *Corros. Sci.*, vol. 41, no. 4, pp. 759–771, 1999.

[54] S. T. Amaral and I. L. Müller, "Electrochemical behaviour of iron in NaOH 0.01 mol/L solutions containing variable amounts of silicate," *J. Braz. Chem. Soc.*, vol. 10, no. 3, pp. 214–221, 1999.

[55] C. Wang *et al.*, "Modified chitosan-oligosaccharide and sodium silicate as efficient sustainable inhibitor

Preprints (www.preprints.org) | NOT PEER-REVIEWED | Posted: 14 October 2020

for carbon steel against chloride-induced corrosion," *J. Clean. Prod.*, vol. 238, p. 117823, 2019, doi: 10.1016/j.jclepro.2019.117823.

[56] O. Lopez-Garrity and G. S. Frankel, "Corrosion inhibition of aa2024-t3 by sodium silicate," *Electrochim. Acta*, vol. 130, pp. 9–21, 2014, doi: 10.1016/j.electacta.2014.02.117.

[57] S. K. Mohammed, "Effect Use of Two Chemical Compounds Sodium Nitrate and Sodium Silicate as Corrosion Inhibitor to Steel Reinforcement," *Al-Khwarizmi Eng. J.*, vol. 14, no. 2, pp. 123–128, 2019, doi: 10.22153/kej.2018.11.006.

[58] M. Scottsdale Dreja and D. Poethkow, "Use of nano-particulate colloidal silica as corrosion inhibitor in e.g. aqueous compositions, aerosol on water basis, furniture care, general-purpose cleaner, deodorants, hair spray and glass cleaner." WO, Germany, 2007.

[59] P. Pedeferri, *Corrosion Science and Engineering*. Springer, 2018.

[60] R. S. Barneyback, Jr. and S. Diamond, "Expression and analysis of pore fluids from hardened cement pastes and mortars," *Cem. Concr. Res.*, vol. 11, no. 2, pp. 279–285, 1981, doi: DOI: 10.1016/0008-8846(81)90069-7.

[61] A. D. Davydov, "Analysis of pitting corrosion rate," *Russ. J. Electrochem.*, vol. 44, no. 7, pp. 835–839, 2008, doi: 10.1134/S1023193508070100.

[62] J. J. Thomas, D. Rothstein, H. M. Jennings, and B. J. Christensen, "Effect of hydration temperature on the solubility behavior of Ca-, S-, Al-, and Si-bearing solid phases in Portland cement pastes," *Cem. Concr. Res.*, vol. 33, no. 12, pp. 2037–2047, Dec. 2003, doi: 10.1016/S0008-8846(03)00224-2.

[63] A. Kenny and A. Katz, "Characterization of the interfacial transition zone around steel rebar by means of the mean shift method," *Mater. Struct. Constr.*, vol. 45, no. 5, 2012, doi: 10.1617/s11527-011-9786-x.

[64] M. Pourbaix, *Atlas of Electrochemical Equilibria in Aqueous Solutions*, 2nd ed. Pergamon Press, 1966.

[65] A. Kenny and A. Katz, "Steel-concrete interface influence on chloride threshold for corrosion – Empirical reinforcement to theory," *Constr. Build. Mater.*, vol. 244, 2020, doi: 10.1016/j.conbuildmat.2020.118376.

[66] K. Karadakis, V. J. Azad, P. Ghods, and O. B. Isgor, "Numerical Investigation of the Role of Mill Scale Crevices on the Corrosion Initiation of Carbon Steel Reinforcement in Concrete," *J. Electrochem. Soc.*, vol. 163, no. 6, pp. C306--C315, 2016, [Online]. Available: http://jes.ecsdl.org/content/163/6/C306.full.pdf+html.

[67] A. Elsharief, M. D. Cohen, and J. Olek, "Influence of aggregate size, water cement ratio and age on the microstructure of the interfacial transition zone," *Cem. Concr. Res.*, vol. 33, no. 11, pp. 1837–1849, 2003, doi: DOI: 10.1016/S0008-8846(03)00205-9.

[68] U. M. Angst *et al.*, "The steel–concrete interface," *Mater. Struct. Constr.*, vol. 50, no. 2, 2017, doi: 10.1617/s11527-017-1010-1.

[69] A. Behnood, K. Van Tittelboom, and N. De Belie, "Methods for measuring pH in concrete: A review," *Construction and Building Materials*, vol. 105. Elsevier Ltd, pp. 176–188, Feb. 15, 2016, doi: 10.1016/j.conbuildmat.2015.12.032.

[70] A. Kenny, "The micro structure of concrete around embedded steel influence on the chloride threshold for chloride induced corrosion," PhD Thesis Technion - Israel Institute of Technology, 2012.